

Available online at www.sciencedirect.com

ScienceDirect

www.elsevier.com/locate/jmbbm

Research Paper

Designing highly structured polycaprolactone fibers using microfluidics

Farrokh Sharifi^a, Diamant Kurteshi^a, Nastaran Hashemi^{a,b,*}^aDepartment of Mechanical Engineering, Iowa State University, Ames, IA 50011, USA^bCenter for Advanced Host Defense Immunobiotics and Translational Comparative Medicine, Iowa State University, Ames, IA 50011, USA

ARTICLE INFO

Article history:

Received 29 October 2015

Received in revised form

2 April 2016

Accepted 5 April 2016

Available online 20 April 2016

Keywords:

Polymer microfibers

Microfluidic approach

Hydrodynamic focusing

Polycaprolactone

ABSTRACT

Microfibers are becoming increasingly important for biomedical applications such as regenerative medicine and tissue engineering. We have used a microfluidic approach to create polycaprolactone (PCL) microfibers in a controlled manner. Through the variations of the sheath fluid flow rate and PCL concentration in the core solution, the morphology of the microfibers and their cross-sections can be tuned. The microfibers were made using PCL concentrations of 2%, 5%, and 8% in the core fluid with a wide range of sheath-to-core flow rate ratios from 120:5 $\mu\text{L}/\text{min}$ to 10:5 $\mu\text{L}/\text{min}$, respectively. The results revealed that the mechanical properties of the PCL microfibers made using microfluidic approach were significantly improved compared to the PCL microfibers made by other fiber fabrication methods. Additionally, it was demonstrated that by decreasing the flow rate ratio and increasing the PCL concentration, the size of the microfiber could be increased. Varying the sheath-to-core flow rate ratios from 40:5 to 10:5, the tensile stress at break, the tensile strain at break, and the Young's modulus were enhanced from 24.51 MPa to 77.07 MPa, 567% to 1420%, and 247.25 MPa to 539.70 MPa, respectively. The porosity and roughness of microfiber decreased when the PCL concentration increased from 2% to 8%, whereas changing the flow rate ratio did not have considerable impact on the microfiber roughness.

© 2016 Elsevier Ltd. All rights reserved.

1. Introduction

Fiber systems are becoming increasingly important for numerous biological applications, such as tissue engineering, as the fibers are able to guide cell growth, alignment, and migration (Chung et al., 2012; Hwang et al., 2008a). Additionally, the design of microfibers gives them the correct

properties in order to perform drug delivery and drug release in the human body for medical purposes (Caplin et al., 2015; Tiwari et al., 2010). The fibers have high surface area-to-volume and strength-to-weight ratios. Some of them are permeable and can be woven into textiles (Boyd et al., 2013b). These properties allow microfibers to carry even delicate materials, such as water-soluble drugs, throughout

*Corresponding author.

E-mail address: nastaran@iastate.edu (N. Hashemi).

a biological medium with good accuracy (Kraitzer et al., 2008; Saraf et al., 2010). This makes for safe insertion and transmittance of material used for treatment, demonstrating the effectiveness of microfibers in medicine. The method of generation of the microfibers plays a role in determining its viability in these types of applications.

Several approaches exist for the fabrication of microfibers from naturally derived or synthetic materials such as electrospinning, wet spinning, biospinning, melt spinning, and the microfluidic techniques (Tamayol et al., 2013). Electrospinning is relatively a simple method and it is feasible to efficiently scale-up and control the involved parameters such as flow rate and voltage. However, there are some difficulties in the fabrication of thick, complex 3D scaffolds with this method (Deng et al., 2012; Hwang et al., 2008a). Additionally, electrospun microfibers are generally not easy to align and it requires extra care to ensure that the fibers are accurately aligned, especially because the randomly aligned fibers are not desirable for applications like growing nerve cells (Jung et al., 2009). Wet spinning is an efficient method for fabricating fibers with a wide range of diameters by changing the needle(s) diameter. Nevertheless, long exposure to chemicals during the fabrication process is required, which can be harmful to cells (Enea et al., 2011). Biospinning method is the process of fabricating silk fibers by insects. Silk has high tensile strength and is biodegradable. In addition, after chemical processing, it is non-cytotoxic and non-inflammatory. The major challenges of using biospun fibers are the limitation of resources, which makes it difficult for the scale-up process, as well as the fact that the process of silk fiber fabrication is time consuming (Reddy and Yang, 2010). In the melt spinning approach, various synthetic polymers can be used for fiber fabrication with this method. Fibers created by melt spinning have high mechanical properties. However, the melt spinning process is in a high temperature range (150–300 °C) and requires using expensive equipment. Using high temperatures during the fiber fabrication process prevents the cell or protein from being loaded onto the fiber in order to deliver the bioactive molecules in biomedical applications (Ella et al., 2011). Additionally, because the viscosity of the melted polymer is relatively high, a high pressure difference is needed to move the melted polymer through the spinneret (Akbari et al., 2011; Yim et al., 2006).

Using microfluidics to fabricate fiber is a relatively new approach in which the fiber is created in a microchannel using coaxial flow of core (pre-polymer) and sheath fluids. The key benefits of using this method include versatility of size, continuity of the fiber fabrication process, and simplicity of cell, protein or drug incorporation. This process is straightforward, cost-efficient, reproducible, and suitable for many biological applications since the fiber is created without using high temperature, high pressure, high voltages, or toxic materials. By changing the flow rate and flow rate ratio, the fiber size and aspect ratio can be simply controlled (Bai et al., 2014; Daniele et al., 2013; Goodrich et al., 2015; Hwang et al., 2008a). The microfluidic fiber fabrication can be employed to create fibers with various materials using different cross-linking mechanisms such as photopolymerization (e.g., poly(ethylene glycol) diacrylate, 4-hydroxybutyl acrylate) (Daniele et al., 2014a, 2014b; Jeong et al., 2004; Oh et al., 2006), ionic gelation (e.g., alginate) (Shin et al., 2007), and thermal phase

transition (e.g., agar) (Khademhosseini et al., 2006; Vunjak-Novakovic et al., 2004). However, there are some studies which employ phase inversion process instead of cross linking method to solidify the polymer (Bai et al., 2014; Hwang et al., 2008a). Hwang et al. (2008a) used the solution of poly(lactic-co-glycolic acid) (PLGA) in dimethyl sulfoxide (DMSO) and mixture of glycerin and distilled water as the core and sheath fluids, respectively. At the fluid–fluid interface in the channel, the DMSO in the core fluid is replaced by water in the sheath fluid and the polymer is solidified. Likewise, Bai et al. (2014) dissolved gelatin in DMSO and showed that by exchanging the DMSO in the core fluid and ethanol in the sheath fluid, the gelatin can be solidified.

This approach makes it feasible to fabricate fibers with different shapes of solid (Bai et al., 2014; Daniele et al., 2013; Hasani-Sadrabadi et al., 2013), tubular (Choi et al., 2011; Kang et al., 2011), hybrid (Jung et al., 2009), and flat (Boyd et al., 2013a; Cho et al., 2012) dimensions for divergent applications such as cell encapsulation, alignment, and immobilization. There are different physical and chemical methods for solidification of fibers including diffusion-limited solidification by solvent extraction, diffusion-limited solidification by chemical cross-linking, and photo polymerization (Bai et al., 2014; Choi et al., 2011; Daniele et al., 2015; Yoo et al., 2015, 2012). The fibers fabricated by photopolymerization are not easily degraded and metabolized in biomedical applications. In addition, ultraviolet radiation (UV) has damaging effects on bioactive species (Jun et al., 2014). It was demonstrated by Hwang et al. (2008b) that the concentration of photo-initiator has adverse impacts on the cell viability. The negative aspects of UV-light can be minimized by decreasing the exposure time and using less-harmful wavelengths than the standard one (Panda et al., 2008). Due to these limitations, photopolymerization is not the most desired approach for fabrication of fibers in cell encapsulation applications.

Although some thermoplastic polymers have been used in microfluidic fiber fabrication such as PLGA (Hwang et al., 2008a) and poly(methyl methacrylate) (PMMA) (Thangawong et al., 2009), there is no report on microfluidic fabrication of PCL fibers. PCL is a Food and Drug Administration (FDA) approved polymer which is widely used as a biomaterial due to its biocompatibility and biodegradability (Acar et al., 2014; Li et al., 2014; Soliman et al., 2010). Due to slower degradation rate of this polymer, for instance compared to PLGA, it possesses no adverse impacts on cell viability and migration because it does not change the PH of the environment during the degradation sharply (Sung et al., 2004). This polymer also has good mechanical properties, is not toxic, and its rate of degradation can be controlled. Furthermore, PCL does not trigger immune responses in the body (Hong and Kim, 2013).

In this paper, we have employed solvent extraction to fabricate biocompatible and biodegradable PCL microfibers in a microfluidic platform for the first time. PCL grants us the advantage of having a biocompatible and strong material from which to make fibers. Using microfluidics, we are able to avoid the constraints of other methods such as electrospinning (Hwang et al., 2008a). We can produce fibers with different cross-sectional shapes while the fabrication is continuous and stops only when the core and sheath solutions stop flowing. By fabricating PCL using a microfluidic microchannel, we are

benefitting from combining the properties of a proven biocompatible material and the unique properties of a microfluidic fabrication technique to create fibers for many biomedical applications such as tissue engineering and drug delivery.

After solidification of PCL fibers, they exit the channel directly into a water bath where the sheath fluid is washed off. The fibers are then collected and characterized to understand their physical and mechanical properties. We have also performed simulations using COMSOL multiphysics to compare with the experimental results.

2. Materials

Polycaprolactone ($M_n=80,000$) and polyethylene glycol (PEG) ($M_n=20,000$) were obtained from Sigma Aldrich (St. Louis, MO). The solvent for the core solution is 2,2,2-trifluoroethanol (TFE), which was purchased from Oakwood Chemical (West Columbia, SC). The material used for the microfluidic channel is polydimethylsiloxane (PDMS). The core solution was prepared by pouring PCL into the TFE at different concentrations by volume (2%, 5%, and 8% PCL). The sheath fluid was made using a PEG concentration of 5% into a mixture of water and ethanol with a volume ratio of 1:1. The solutions were prepared at room temperature. The syringes used to pump the fluids were obtained from BD Medical (Franklin Lakes, New Jersey). The syringe pumps used to introduce fluids to the microchannel were purchased from Cole Parmer (Vernon Hills, Illinois).

3. Microfluidic approach

Using a dual-drive syringe pump, the core and sheath fluids are simultaneously introduced into the microchannel. The core fluid enters the channel through the central opening and the sheath flow enters on each of the sides. Additionally, our microchannel contains three inlets, one in the middle for introducing the core flow and two on the sides for running sheath flows. (Fig. 1). The shear force between the core and sheath fluids focuses the core fluid in the center of the microchannel hydrodynamically (Asrar et al., 2015; Hashemi et al., 2011a, 2011b, 2010) and fibers are formed from the core fluid employing solvent extraction solidification approach. The microfluidic method enables the fabrication of fibers with different sizes and cross sections. The dimensions of the fiber depend on the core and sheath flow rates (Zarrin and Dovichi, 1985). Additionally, the shear force aligns the polymer chains along the flow direction in the final microfiber product. Therefore, we can control the microstructures of the fibers and their bulk mechanical properties. Here, the phase inversion process causes the TFE in the core fluid to be replaced by the sheath fluid. Because PCL does not dissolve in the sheath fluid, it becomes solidified as a microfiber further downstream the channel.

Fig. 1(a) illustrates a schematic of microfluidic fiber fabrication. More details about the design of the microchannels are provided in Figs. S1 and S2. The pattern of the core fluid at different sections of the channel is illustrated by Fig. 1(b). In fact, the sheath fluid has a lateral hydrodynamic force on the

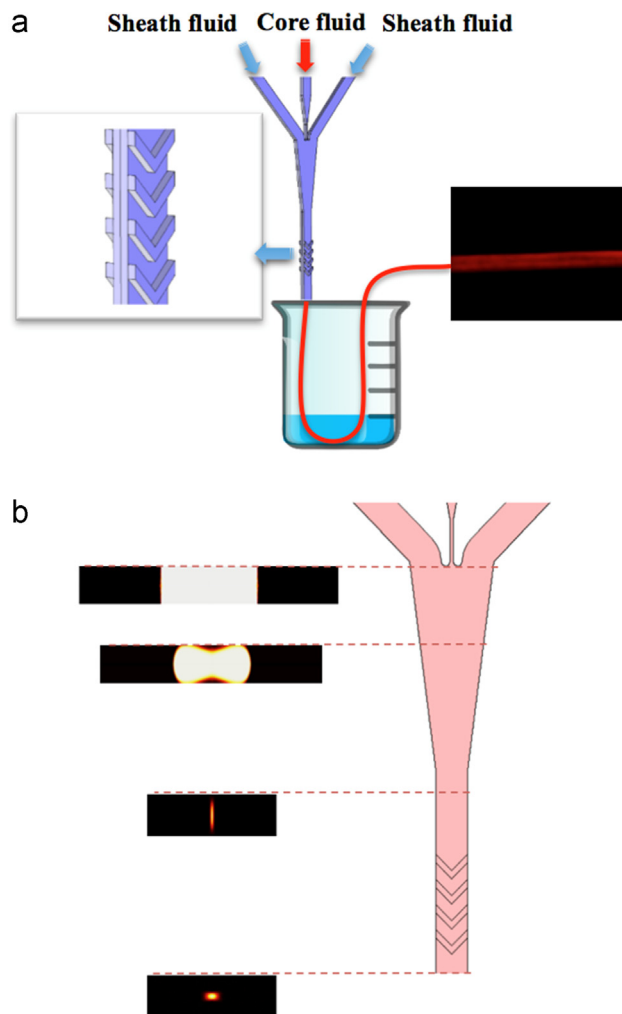


Fig. 1 – (a) A schematic of microfluidic fiber fabrication method. (b) Concentration pattern of the core fluid at different sections of the channel; the flow rate ratio of 80:5 $\mu\text{L}/\text{min}$ for the sheath and core fluids, respectively.

core fluid in the nozzle area. After that, the cross section of the channel remains constant until two fluids meet the chevrons of the channel. In this region, the hydrodynamic resistance in the direction parallel to the peaks and valleys is less than the direction of the channel. Consequently, the component of velocity which is perpendicular to the channel increases for both of the fluids. The hydrodynamic resistance is inversely proportional to the flow rate. Therefore, the sheath fluid will experience less resistance compared to the core fluid since the flow rate of the sheath fluid is considerably higher than the core fluid. Sheath fluid wraps around the core fluid and exerts vertical hydrodynamic force towards the center of the channel in the chevrons region. After passing through these chevrons, the core fluid will be focused at the center of the channel and there will not be any contact between the core fluid and the channel walls. Apart from exerting hydrodynamic force, the sheath fluid plays the role of a lubricant in the channel to facilitate fiber extrusion. Therefore, the viscosity of the sheath fluid should be matched to that of the core fluid. For this purpose,

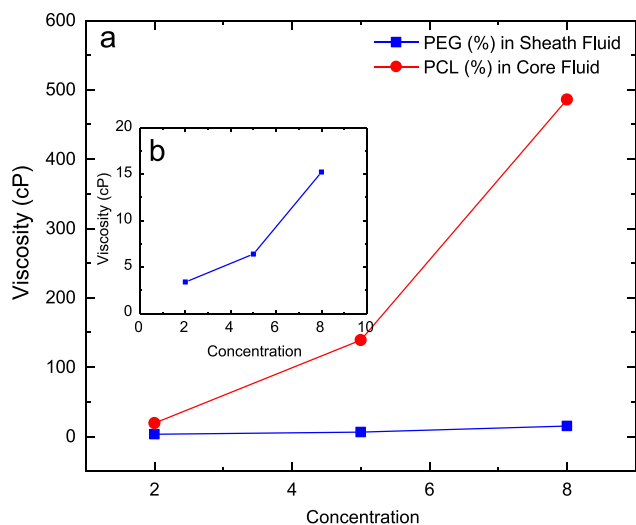


Fig. 2 – Viscosity of (a) the core and sheath solutions using different concentrations of PCL and PEG, respectively; (b) enlarged view of sheath solution viscosity made by three different concentrations of PEG.

polyethylene glycol (PEG) is added to the sheath fluid in order to increase its viscosity. Fig. 2 shows the viscosity of core and sheath fluids at different concentrations of PCL and PEG (2–8%), respectively. While the range of viscosity varies from 19 cP to 500 cP for the core fluid, it is limited to 2–16 cP for the sheath fluid. In this study, we used 5% PEG in the sheath fluid and changed the concentration of the PCL in the core fluid from 2% to 8% in order to show the versatility of microfluidic approach in fabricating fiber using a wide range of core fluid viscosity.

While the core flow rate is kept constant at 5 $\mu\text{L}/\text{min}$, the sheath flow rate varies from 10 $\mu\text{L}/\text{min}$ to 120 $\mu\text{L}/\text{min}$. Our microchannel contains three inlets, one in the middle for introducing the core flow and two on the sides for running sheath flows. The channel has four chevron grooves that create vertical hydrodynamic force. The magnitude of the hydrodynamic force is directly related to the flow rate ratio (velocity gradient between sheath and core fluid), which is an important parameter in determining the features of the fiber.

Downstream from the microchannel entrance, the fluid comes into contact with the chevron grooves, which are engrained on the top and bottom surfaces of the channel. The grooves play an important role in focusing the core fluid vertically and determining the final cross-sectional shape of the fibers. The shear stress aligns the polymer chains in the core flow in the direction of the flows. The solidification of core flow occurs once it comes to contact with the sheath flows. During the whole process, the channel is positioned vertically and the resulting fibers exit directly into a water bath.

After the fibers were recovered, their characteristics were evaluated through several means. A scanning electron microscope (SEM) from Nikon (Tokyo, Japan) was used to determine the morphology of the fibers. The SEM was used to study the effects of changing the flow rate ratio of sheath and core fluids as well as the PCL concentration in the core solution on

the morphology and cross section of the fabricated microfibers. In addition, the mechanical properties of the fibers were measured to assess their strength. Finally, the microfluidic fiber fabrication was simulated using COMSOL multi-physics software in order to compare the experimental and numerical results.

4. Characterization

The morphology and cross section of the microfibers were studied using the field emission scanning electron microscopy (FE-SEM) (JSM-6700F at an acceleration voltage of 5 kV). The viscosities of the core and sheath solutions were measured using a digital viscometer (DV-E, Brookfield Engineering Laboratories, Inc., Middleboro, MA). For measuring the stress-strain behavior of the fibers, single fiber was tested using Instron Universal Testing machine (Model 5569, Instron Engineering Corp., Canton, MA). For each type of the fibers, 10 samples were tested and the average values for each type were reported. Since the PCL fibers have high ductility, we used a 10 N load cell to get enough resolution, and the extension rate was set to 20 mm/min. In this test, the samples were prepared by attaching them on a paper frame in order to be gripped properly by the Instron machine (Fig. S3). After mounting the sample on the machine, we cut two sides of the frame to get the mechanical properties of PCL fiber. The length of the samples for this test was 15 mm. The results were found using Bluehill software. A video file is provided in supplementary materials, that shows high ductility of the fiber during the tensile test. The stress-strain curves were fitted with linear line for the elastic region. Second order polynomial equation was used for the plastic region because its coefficient of determination (R-Square) was better compared to the linear line for all of the data.

Supplementary material related to this article can be found online at <http://dx.doi.org/10.1016/j.jmbbm.2016.04.005>.

5. Results and discussion

We fabricated microfibers using 2%, 5%, and 8% PCL and 5% PEG in TFE and water/ethanol (with the volume ratio of 1:1), respectively. Varying the sheath and core flow rates, it was found that the core flow rate of 5 $\mu\text{L}/\text{min}$ and the sheath flow rate of 10–120 $\mu\text{L}/\text{min}$ are appropriate flow rates in order to obtain continuous microfiber.

The versatility of the microfluidic fiber fabrication method can be highlighted by using various flow rates of sheath fluid and PCL concentrations in the core fluid. The results revealed that the flow rate ratio of the core and sheath fluids plays a significant role in the morphology of the fabricated fibers. Using a very low sheath flow rate does not allow for enough of both the vertical and horizontal hydrodynamic forces on the core fluid. As a result, the width of the core fluid increases. Also, the aggregation of the polymer becomes stronger than its elongation along the channel. This condition leads to occurrence of clogging in the microchannel. On the other hand, if the core fluid has a high flow rate, there is a possibility that the core fluid exit the channel and no

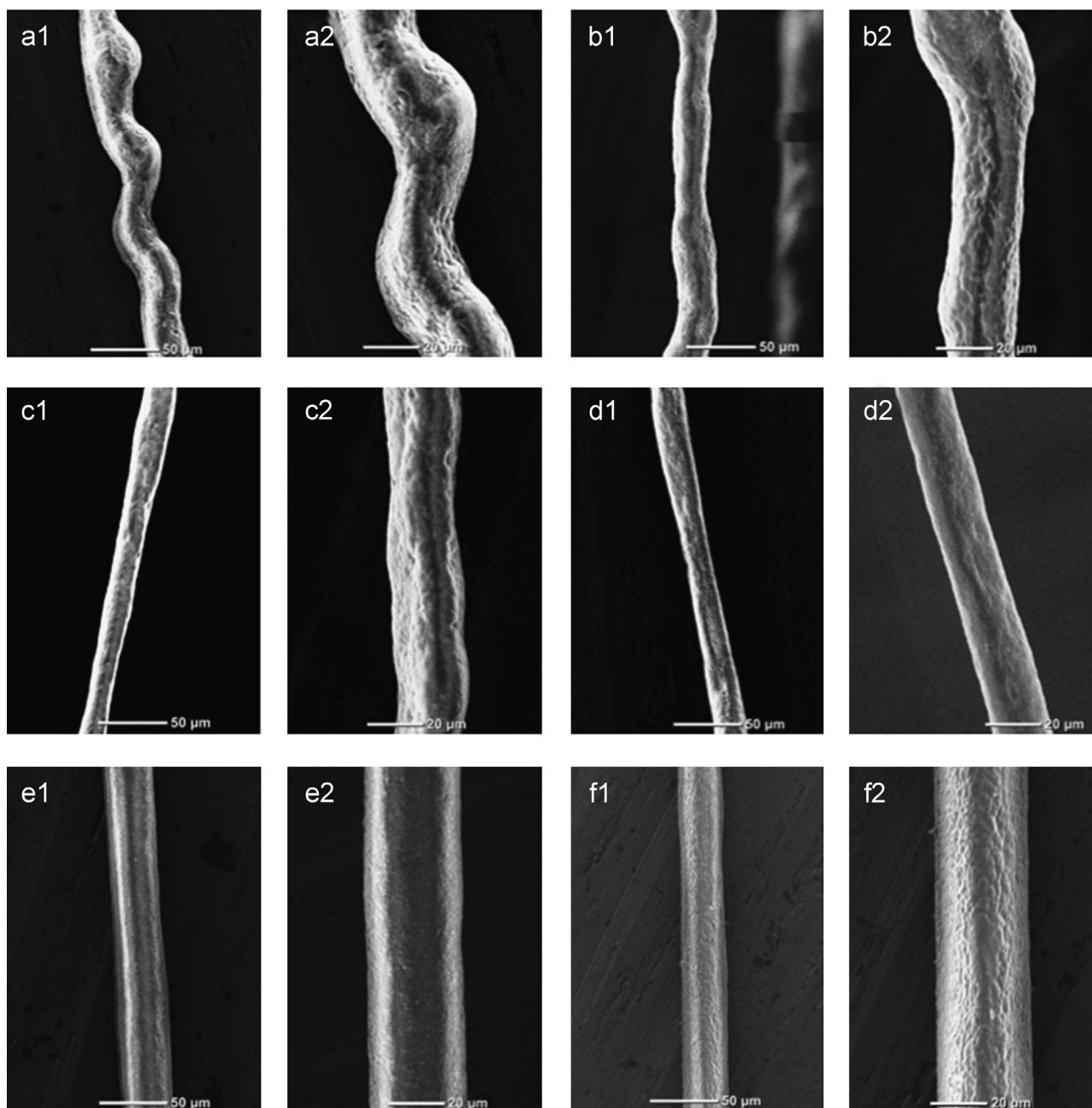


Fig. 3 – SEM images of PCL microfibers with 5% PCL in TFE (core fluid) and 5% PEG in water and ethanol (sheath fluid) and different flow rates of (a) 120: 5 (b) 100: 5 (c) 80: 5 (d) 60: 5 (e) 20: 5, and (f) 10: 5 $\mu\text{L}/\text{min}$ for the sheath and core fluids, respectively.

solidification happens. Fig. 3 shows the SEM images of the representative microfibers obtained using different flow rate ratios. The concentrations of PCL and PEG were kept at a constant value of 5% in the core and sheath fluids, respectively.

This figure illustrates that the roughness of the surface is not significantly affected by changing the flow rate ratio between the fluids. However, at the higher flow rates of sheath fluid, the microfibers have wavy structures, and as the sheath flow rate decreases, the microfibers tend to be more uniform and straight. This means that the Kelvin-Helmholtz instability occurs at high flow rate ratios due to

sharp difference of velocities at the core fluid/sheath fluid interface in the channel, and it leads to the creation of wavy shaped microfibers. Additionally, this figure demonstrates that the size of the microfibers increases when the sheath flow rate reduces. This is expected, because when the difference of the velocities decreases, the hydrodynamic shear force exerted from the sheath fluid on the core fluid weakens. Consequently, the core fluid expands in the channel and the average diameter of the fiber increases.

In Fig. 4(a)–(c), the cross-sectional SEM images of the microfibers fabricated with different flow rate ratios are provided. This figure shows that the cross-section of the

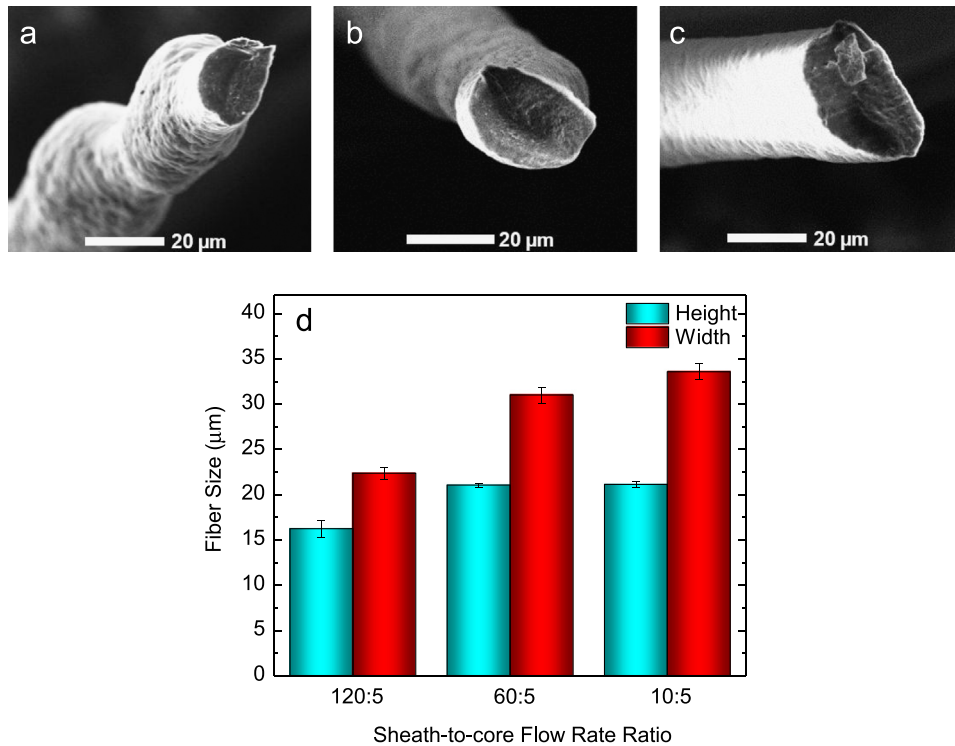


Fig. 4 – Cross sectional SEM images of PCL microfibers with 5% PCL in TFE (core fluid) and 5% PEG in water and ethanol (sheath fluid) fabricated by sheath and core flow rates of (a) 120:5, (b) 60:5, and (c) 10:5 μL/min, respectively. (d) Dimensions of the PCL fibers fabricated using different sheath-to-core flow rate ratios.

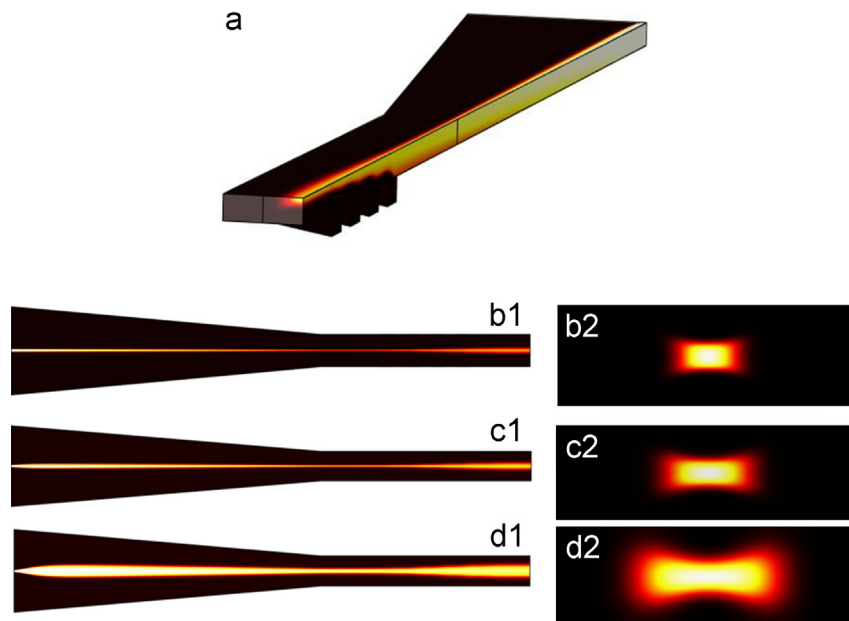


Fig. 5 – (a) Three-dimensional concentration distribution of core fluid in sheath fluid along the channel; the flow rate ratio is 80:5 μL/min for the sheath and core fluids, respectively; Top view of the channel and the cross section of the fibers with sheath and core flow-rates of (b₁) and (b₂) 120:5, (c₁) and (c₂) 60:5, and (d₁) and (d₂) 10:5 μL/min, respectively. (For interpretation of the references to color in this figure, the reader is referred to the web version of this article)

fibers made by microfluidic approach can be tuned by simply changing the flow rate ratio between the sheath and core fluids. Additionally, the dimensions of the fibers (average ± standard error) are shown in Fig. 4(d). The width and height of

the PCL fiber at the sheath-to-core flow rate ratio of 120:5 are 16.21 μm and 22.34 μm, respectively. The decrease of the flow rate ratio to 10:5 increases both the width and height of the fiber to 21.12 μm and 33.56 μm, respectively. Moreover, the

aspect ratio of the fiber increases by a factor of 1.15 when the flow rate ratio reduces from 120:5 to 10:5. That was expected because when the flow rate ratio between two fluids diminishes, the lateral hydrodynamic force exerted to the core fluid by sheath fluid weakens. Consequently, the core fluid has more freedom to grow in the lateral direction. On the other hand, when the sheath flow rate increases, the shear force intensifies and the core fluid is stretched more due to the higher hydrodynamic force that leads to the fabrication of fibers with smaller size.

The microfluidic fiber fabrication was simulated using COMSOL multiphysics. The Navier–Stokes equation for incompressible flow at steady state was used to numerically solve the momentum balance. Because the inertial forces are negligible at low Reynolds number, the motion of the fluid can be approximately described by the reversible Stokes equation in which the nonlinear term can be neglected. We used Fick's law, $-\nabla \cdot (-D \cdot \nabla c) + u \cdot \nabla c = 0$, to describe the diffusive transport in the micro-channel. In this equation, D is the diffusion coefficient and c represents the concentration. The Navier–Stokes equation was solved first and was then

followed by the convection–diffusion relationships. Due to symmetry, one fourth of the channel was modeled. The velocity in different sections of the channel is provided in Fig. S2. This figure illustrates that the velocity of two fluids increases by passing through the nozzle part of the channel. In the chevrons area, the component of velocity which is perpendicular to the channel, increases by passing the fluid through the chevrons. Fig. 5(a) shows the concentration distribution along the channel. The bright and dark colors represent the situations of core and sheath fluids, respectively along the channel. Therefore, the effects of lateral and vertical hydrodynamic focusing forces of the sheath fluid on the core fluid can be observed clearly by following the brighter color along the channel. Additionally, the bright color at the output of the microchannel represents the cross sectional pattern of the microfiber fabricated using a specific flow rate ratio. Based on Fig. 5(a), the thickness of the core fluid reduces after the nozzle area, which reveals an increasing lateral force of the sheath fluid on the core fluid. Downstream from the initial focusing region, the series of chevrons change the hydrodynamic resistance in the channel such

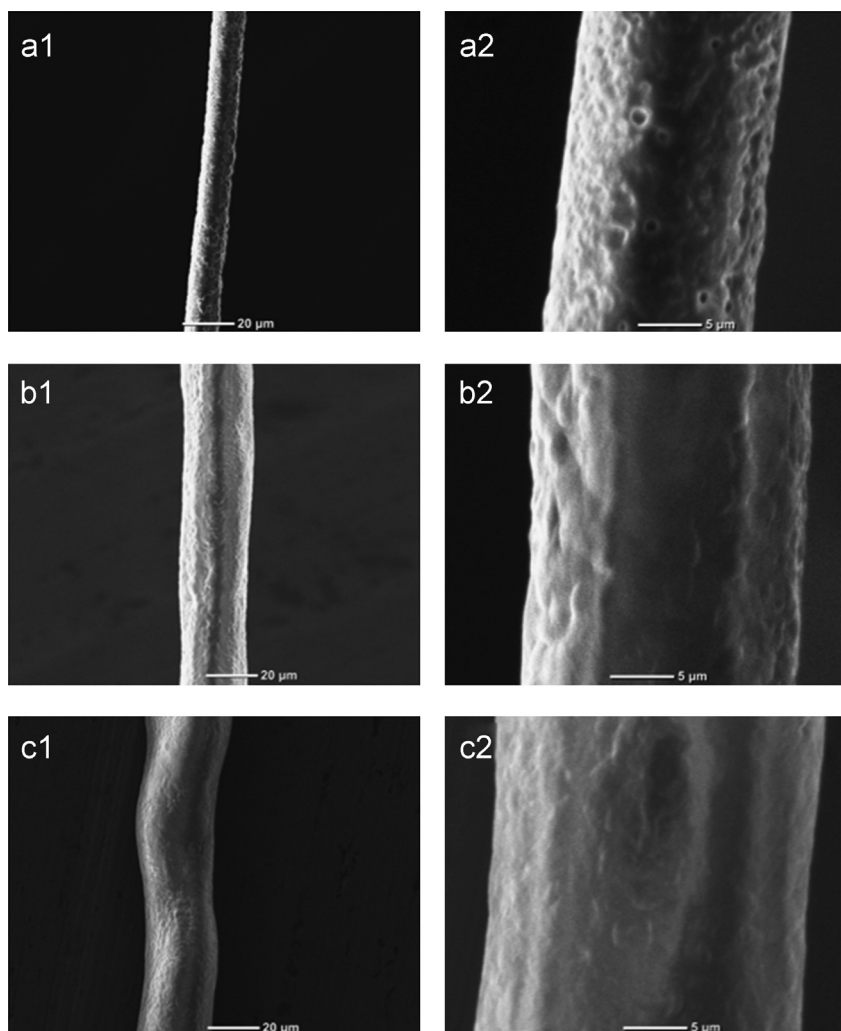


Fig. 6 – SEM images of PCL microfibers with 5% PEG in the sheath fluid and the PCL concentrations of (a₁) and (a₂) 2%; (b₁) and (b₂) 5%; and (c₁) and (c₂) 8% in the core fluid. Sheath flow rate is 60 μL/min and core flow rate is 5 μL/min.

that the resistance in the perpendicular direction becomes smaller than the parallel one. Fig. 5(a) displays that the vertical force in the chevrons region gradually focuses the core solution at the center of the channel.

The concentration distribution of the core and sheath fluids are shown in Fig. 5(b1)–(d1) for different values of sheath flow-rate and constant value of 5 $\mu\text{L}/\text{min}$ for the core flow rate. This figure illustrates a weakening of the hydrodynamic lateral force of the sheath fluid on the core fluid due to decreasing the sheath flow-rate. Consequently, the width of the fabricated fiber becomes larger. The vertical hydrodynamic force, however, does not change significantly due to the fact that this force is originated from the number of the chevrons. Therefore, the combination of a decrease in lateral force and a constant value of the vertical force leads to the development of the ribbon-shape pattern. Fig. 5(b2)–(d2) illustrates the trend in which the core cross section changes to a ribbon-shaped pattern. These results demonstrated consistency between the experimental and numerical results.

The concentration of the core fluid can be changed in microfluidic fiber fabrication as well as the flow rate and flow rate ratio between the sheath and core fluid in order to change the characteristics of microfibers. Fig. 6 illustrates the effects of different concentrations (2%, 5%, and 8%) of PCL in the core fluid on morphology of fibers. Increasing the PCL concentration results in fiber with smoother surface. Additionally, 2% PCL fibers show more porosity compared to the fibers made from higher PCL concentrations. When core fluid with low concentration of PCL is introduced into the channel, the total amount of PCL in core fluid is not enough to create a

uniform fiber after solvent extraction and the resulting fibers become more porous. Moreover, the higher roughness and existence of porosity on the fiber at low concentrations of PCL is due to rapid exchange of TFE and sheath fluid compared to higher concentrations. While the uniform microfibers have higher mechanical properties, more porous microfibers can enhance cell adhesion and cell proliferation, which are desirable in tissue engineering applications. Furthermore, tuning the porosity and microstructures of the fibers by changing the PCL concentration in the core fluid is another advantage of microfluidic approach. The cross-sectional SEM images of PCL microfibers fabricated using different percentages of PCL in the core fluid are shown in Fig. 7(a)–(c). This figure demonstrates that the PCL concentration can influence the size of the resulting fiber as well as the flow rate ratio between the two fluids. Fig. 7(d) displays the dimensions of the fibers made by different PCL concentration in the core fluid. We observed that the dimension of the fiber (width \times height) increases from 20.1 $\mu\text{m} \times 13.3 \mu\text{m}$ to 33.65 $\mu\text{m} \times 24.25 \mu\text{m}$ when the PCL concentration changes from 2% to 8%, while the aspect ratio does not change significantly. That is because when lower amount of PCL in the core solution flows through the channel, the dimensions of PCL solidified as a fiber during the phase inversion process in the microchannel will be reduced.

The mechanical properties of the fibers made by different flow rate ratios were investigated. Fig. S3 illustrates a single fiber prepared for the tensile test. Stress–strain behavior of different fibers are shown in Fig. 8(a). This figure demonstrates a wide range of mechanical properties that can be obtained

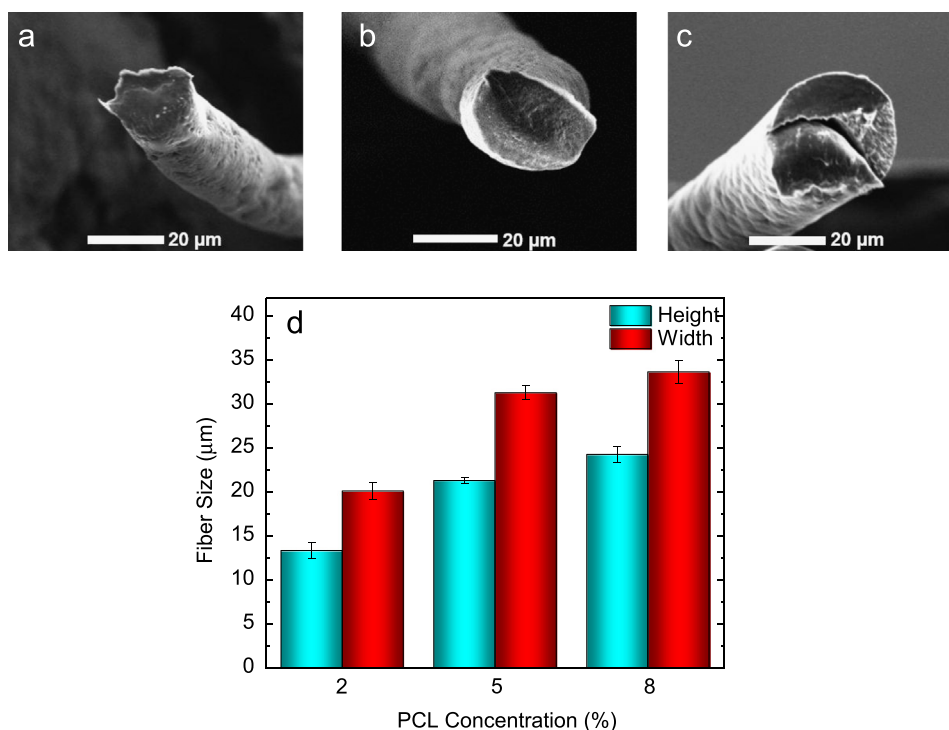


Fig. 7 – Cross sectional SEM images of PCL microfibers with different concentrations of (a) 2%; (b) 5%; and (c) 8% PCL in the core fluid and 5% PEG in the sheath fluid with the flow rate of 60:5 $\mu\text{L}/\text{min}$ for the sheath and core fluids, respectively. (d) Dimensions of the PCL fibers fabricated using different PCL concentrations in the core fluid.

using this microfluidic approach. As expected from a typical plastic material, the elastic region of the PCL stress–strain curve is in a small range, which is shown in Fig. 8(b). The Young's modulus of the fibers are shown in Fig. 8(c). Additionally, yield strain (%), yield stress (MPa), Young's modulus (MPa), strain at break (%), and stress at break (MPa) are listed in Table 1 for different PCL microfibers. The results show that the decrease of the flow rate ratio from 40:5 to 10:5, significantly improves the tensile stress at break, tensile strain at break,

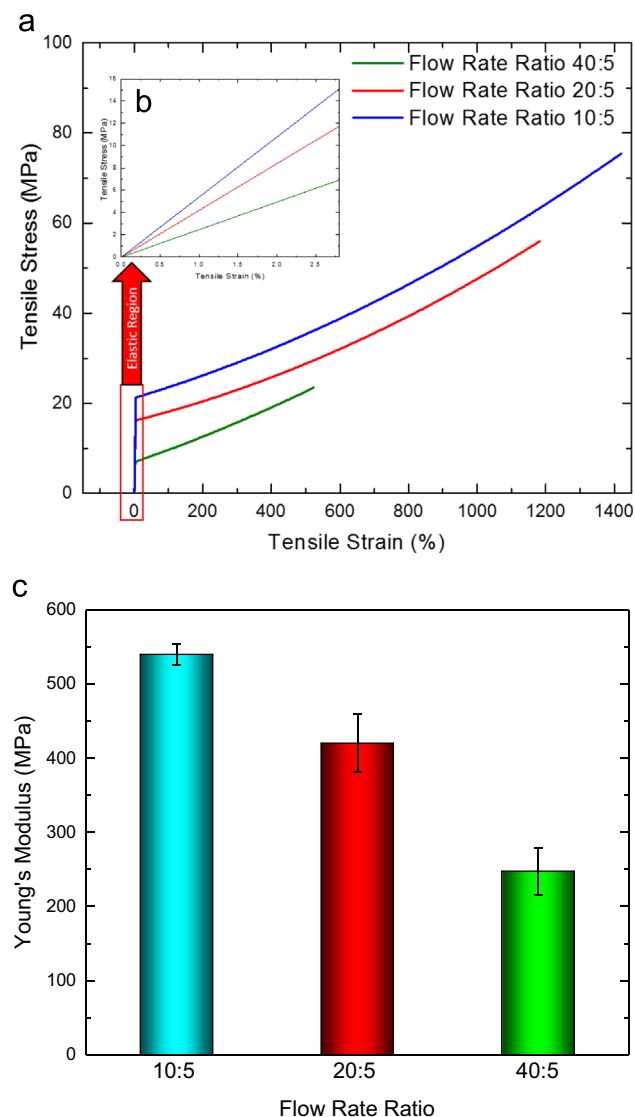


Fig. 8 – (a) Tensile stress–strain behavior, (b) enlarged view of the elastic region of stress–strain curve, and (c) Young's modulus of PCL microfibers fabricated with different flow rate ratios with the PCL concentration of 5% in TFE.

and the Young's modulus from 24.51 MPa to 77.07 MPa, 567% to 1420%, and 247.25 MPa to 539.70 MPa, respectively. The yield stress (MPa) and yield elongation (%) improve by a factor of 3.33 and 1.45 when the flow rate ratio decreases from 40:5 to 20:5.

Although the mechanical properties of electrospun PCL fibrous scaffold widely have been studied, there are few reports about the mechanical properties of PCL single fibers made by electrospinning method. It was found that the reported values of the tensile strain at break (%) for electrospun fibers are significantly lower than our results (Baker et al., 2016; Croisier et al., 2012; Duling et al., 2008; Ghasemi-Mobarakeh et al., 2008; Sing Yian et al., 2006). This could be due to the microstructure organization of the fibers as the shear stress plays a pivotal role in aligning the polymer chains in the direction of the flow and consequently creating highly structured fibers. However, the values of stress at break and Young's modulus obtained in this study are comparable with the ones reported for the electrospun PCL fibers. Also based on the SEM images of microfiber cross sections shown in Fig. 4, decreasing the flow rate ratio leads to an increase in the size and aspect ratio of the fiber cross section such that the fiber cross section tends to have a ribbon shape. Consequently, this improvement in mechanical properties of microfibers can be due to the ribbon shape of the microfiber cross-section.

6. Conclusions

PCL microfibers with improved mechanical properties were fabricated using the microfluidic fiber fabrication. Employing microfluidic fiber fabrication approach, we created microfibers with the maximum strain of 1420%. We showed through SEM that the morphology and size of the fibers could be controlled by varying the PCL percentage in the core solution and the flow rate ratio of sheath to core fluids. While the smoothness of the fiber was improved by increasing the PCL concentration in the core solution from 2% to 8%, the flow rate ratio did not have a substantial influence on the roughness of the fiber. The aspect ratio of the fiber increases by diminishing the flow rate ratio because when the sheath flow rate decreases, the core fluid expands in the channel, which increases the width of the fiber. Numerical simulations were consistent with the experimental results. This development in size and cross section of the fiber enhanced the mechanical properties of the microfiber. These are the most improved properties compared to those of the previous reports about PCL fibers created using other fabrication methods. This improvement reveals unique capability of microfluidic platform to create fibers with a wide range of mechanical

Table 1 – Mechanical properties of PCL fibers made by different sheath-to-core flow rate ratios.

Flow rate ratio	Yield strain (%)	Yield stress (MPa)	Young's modulus (MPa)	Strain at break (%)	Stress at break (MPa)
40:5	2.70±0.65	6.02±1.02	247.25±32.08	567±61.24	24.51±3.11
20:5	3.78±0.24	15.78±1.50	420.03±38.89	1079.25±63.20	57.35±5.46
10:5	3.92±0.33	20.05±1.15	539.70±14.50	1420.4±79.47	77.07±5.64

properties simply by changing the fabrication parameters such as flow rate ratio and viscosity.

Acknowledgments

This work was funded in part by the Office of Naval Research Grant N000141612246, Iowa State University Presidential Initiative for Interdisciplinary Research, and U.S. Department of Energy Office of Science under the Science Undergraduate Laboratory Internship (SULI) Program at Ames Laboratory. The authors also would like to take the opportunity to express their appreciation to Jeremy Caplin, Rui Ding, and Michelle Grawe for their assistance in this research.

Appendix A. Supplementary material

Supplementary data associated with this article can be found in the online version at <http://dx.doi.org/10.1016/j.jmbbm.2016.04.005>.

REFERENCES

- Acar, H., Çınar, S., Thunga, M., Kessler, M.R., Hashemi, N., Montazami, R., 2014. Study of physically transient insulating materials as a potential platform for transient electronics and bioelectronics. *Adv. Funct. Mater.* 24, 4135–4143.
- Akbari, M., Sinton, D., Bahrami, M., 2011. Viscous flow in variable cross-section microchannels of arbitrary shapes. *Int. J. Heat Mass Transf.* 54, 3970–3978.
- Arsar, P., Sucur, M., Hashemi, N., 2015. Multi-pixel photon counters for optofluidic characterization of particles and microalgae. *Biosensors* 5, 308–318.
- Bai, Z., Reyes, J.M.M., Montazami, R., Hashemi, N., 2014. On-chip development of hydrogel microfibers from round to square/ribbon shape. *J. Mater. Chem. A* 2, 4878–4884.
- Baker, S.R., Banerjee, S., Bonin, K., Guthold, M., 2016. Determining the mechanical properties of electrospun poly-ε-caprolactone (PCL) nanofibers using AFM and a novel fiber anchoring technique. *Mater. Sci. Eng.: C* 59, 203–212.
- Boyd, D.A., Shields, A.R., Howell, P.B., Ligler, F.S., 2013a. Design and fabrication of uniquely shaped thiol-ene microfibers using a two-stage hydrodynamic focusing design. *Lab Chip* 13, 3105–3110.
- Boyd, D.A., Shields, A.R., Naciri, J., Ligler, F.S., 2013b. Hydrodynamic Shaping, polymerization, and subsequent modification of thiol click fibers. *ACS Appl. Mater. Interfaces* 5, 114–119.
- Caplin, J.D., Granados, N.G., James, M.R., Montazami, R., Hashemi, N., 2015. Microfluidic organ-on-a-chip technology for advancement of drug development and toxicology. *Adv. Healthc. Mater.* 4, 1426–1450.
- Cho, S., Shim, T.S., Yang, S.M., 2012. High-throughput optofluidic platforms for mosaicked microfibers toward multiplex analysis of biomolecules. *Lab Chip* 12, 3676–3679.
- Choi, C.H., Yi, H., Hwang, S., Weitz, D.A., Lee, C.S., 2011. Microfluidic fabrication of complex-shaped microfibers by liquid template-aided multiphase microflow. *Lab Chip* 11, 1477–1483.
- Chung, B.G., Lee, K.H., Khademhosseini, A., Lee, S.H., 2012. Microfluidic fabrication of microengineered hydrogels and their application in tissue engineering. *Lab Chip* 12, 45–59.
- Croisier, F., Duwez, A.S., Jerome, C., Leonard, A.F., van der Werf, K. O., Dijkstra, P.J., Bennink, M.L., 2012. Mechanical testing of electrospun PCL fibers. *Acta Biomater.* 8, 218–224.
- Daniele, M.A., Radom, K., Ligler, F.S., Adams, A.A., 2014b. Microfluidic fabrication of multiaxial microvessels via hydrodynamic shaping. *RSC Adv.* 4, 23440–23446.
- Daniele, M.A., Boyd, D.A., Adams, A.A., Ligler, F.S., 2015. Microfluidic strategies for design and assembly of microfibers and nanofibers with tissue engineering and regenerative medicine applications. *Adv. Healthc. Mater.* 4, 11–28.
- Daniele, M.A., Adams, A.A., Naciri, J., North, S.H., Ligler, F.S., 2014a. Interpenetrating networks based on gelatin methacrylamide and PEG formed using concurrent thiol click chemistries for hydrogel tissue engineering scaffolds. *Biomaterials* 35, 1845–1856.
- Daniele, M.A., North, S.H., Naciri, J., Howell, P.B., Foulger, S.H., Ligler, F.S., Adams, A.A., 2013. Rapid and continuous hydrodynamically controlled fabrication of biohybrid microfibers. *Adv. Funct. Mater.* 23, 698–704.
- Deng, M., James, R., Laurencin, C.T., Kumbar, S.G., 2012. Nanostructured polymeric scaffolds for orthopaedic regenerative engineering. *IEEE Trans. Nanobiosci.* 11, 3–14.
- Duling, R.R., Dupaix, R.B., Katsube, N., Lannutti, J., 2008. Mechanical characterization of electrospun polycaprolactone (PCL): a potential scaffold for tissue engineering. *J. Biomech. Eng. Trans. ASME* 130, 13.
- Ella, V., Annala, T., Lansman, S., Nurminen, M., Kellomaki, M., 2011. Knitted polylactide 96/4 L/D structures and scaffolds for tissue engineering: shelf life, in vitro and in vivo studies. *Biomater* 1, 102–113.
- Enea, D., Henson, F., Kew, S., Wardale, J., Getgood, A., Brooks, R., Rushton, N., 2011. Extruded collagen fibres for tissue engineering applications: effect of crosslinking method on mechanical and biological properties. *J. Mater. Sci. Mater. Med.* 22, 1569–1578.
- Ghasemi-Mobarakeh, L., Prabhakaran, M.P., Morshed, M., Nasr-Esfahani, M.-H., Ramakrishna, S., 2008. Electrospun poly(ε-caprolactone)/gelatin nanofibrous scaffolds for nerve tissue engineering. *Biomaterials* 29, 4532–4539.
- Goodrich, P.J., Sharifi, F., Hashemi, N., 2015. Rapid prototyping of microchannels with surface patterns for fabrication of polymer fibers. *RSC Adv.* 5, 71203–71209.
- Hasani-Sadrabadi, M.M., VanDersarl, J.J., Dashtimoghadam, E., Bahlakeh, G., Majedi, F.S., Mokarram, N., Bertsch, A., Jacob, K. I., Renaud, P., 2013. A microfluidic approach to synthesizing high-performance microfibers with tunable anhydrous proton conductivity. *Lab Chip* 13, 4549–4553.
- Hashemi, N., Erickson, J.S., Golden, J.P., Ligler, F.S., 2011b. Optofluidic characterization of marine algae using a microflow cytometer. *Biomicrofluidics* 5, 032009.
- Hashemi, N., Howell, J.P.B., Erickson, J.S., Golden, J.P., Ligler, F.S., 2010. Dynamic reversibility of hydrodynamic focusing for recycling sheath fluid. *Lab Chip* 10, 1952–1959.
- Hashemi, N., Erickson, J.S., Golden, J.P., Jackson, K.M., Ligler, F.S., 2011a. Microflow cytometer for optical analysis of phytoplankton. *Biosens. Bioelectron.* 26, 4263–4269.
- Hong, S.G., Kim, G.H., 2013. Mechanically improved electrospun PCL biocomposites reinforced with a collagen coating process: preparation, physical properties, and cellular activity. *Bioprocess Biosyst. Eng.* 36, 205–214.
- Hwang, C.M., Khademhosseini, A., Park, Y., Sun, K., Lee, S.-H., 2008a. Microfluidic chip-based fabrication of PLGA microfiber scaffolds for tissue engineering. *Langmuir* 24, 6845–6851.
- Hwang, D.K., Dendukuri, D., Doyle, P.S., 2008b. Microfluidic-based synthesis of non-spherical magnetic hydrogel microparticles. *Lab Chip* 8, 1640–1647.
- Jeong, W., Kim, J., Kim, S., Lee, S., Mensing, G., Beebe, D.J., 2004. Hydrodynamic microfabrication via "on the fly" photopolymerization of microscale fibers and tubes. *Lab Chip* 4, 576–580.

- Jun, Y., Kang, E., Chae, S., Lee, S.H., 2014. Microfluidic spinning of micro- and nano-scale fibers for tissue engineering. *Lab Chip* 14, 2145–2160.
- Jung, J.-H., Choi, C.-H., Chung, S., Chung, Y.-M., Lee, C.-S., 2009. Microfluidic synthesis of a cell adhesive Janus polyurethane microfibrillar fiber. *Lab Chip* 9, 2596–2602.
- Kang, E., Jeong, G.S., Choi, Y.Y., Lee, K.H., Khademhosseini, A., Lee, S.H., 2011. Digitally tunable physicochemical coding of material composition and topography in continuous micro-fibers. *Nat. Mater.* 10, 877–883.
- Khademhosseini, A., Langer, R., Borenstein, J., Vacanti, J.P., 2006. Microscale technologies for tissue engineering and biology. *Proc. Natl. Acad. Sci. USA* 103, 2480–2487.
- Kraitzler, A., Ofek, L., Schreiber, R., Zilberman, M., 2008. Long-term in vitro study of paclitaxel-eluting bioresorbable core/shell fiber structures. *J. Control. Release* 126, 139–148.
- Li, Y.-F., Rubert, M., Aslan, H., Yu, Y., Howard, K.A., Dong, M., Besenbacher, F., Chen, M., 2014. Ultraporos interweaving electrospun microfibers from PCL-PEO binary blends and their inflammatory responses. *Nanoscale* 6, 3392–3402.
- Oh, H.J., Kim, S.H., Baek, J.Y., Seong, G.H., Lee, S.H., 2006. Hydrodynamic micro-encapsulation of aqueous fluids and cells via 'on the fly' photopolymerization. *J. Micromech. Microeng.* 16, 285–291.
- Panda, P., Ali, S., Lo, E., Chung, B.G., Hatton, T.A., Khademhosseini, A., Doyle, P.S., 2008. Stop-flow lithography to generate cell-laden microgel particles. *Lab Chip* 8, 1056–1061.
- Reddy, N., Yang, Y.Q., 2010. Structure and properties of cocoons and silk fibers produced by *Hyalophora cecropia*. *J. Mater. Sci.* 45, 4414–4421.
- Saraf, A., Baggett, L.S., Raphael, R.M., Kasper, F.K., Mikos, A.G., 2010. Regulated non-viral gene delivery from coaxial electrospun fiber mesh scaffolds. *J. Control. Release* 143, 95–103.
- Shin, S., Park, J.Y., Lee, J.Y., Park, H., Park, Y.D., Lee, K.B., Whang, C. M., Lee, S.H., 2007. "On the fly" continuous generation of alginate fibers using a microfluidic device. *Langmuir* 23, 9104–9108.
- Sing Yian, C., Todd, C.H., Chwee Teck, L., Kam, W.L., 2006. Mechanical properties of single electrospun drug-encapsulated nanofibers. *Nanotechnology* 17, 3880.
- Soliman, S., Pagliari, S., Rinaldi, A., Forte, G., Fiaccavento, R., Pagliari, F., Franzese, O., Minieri, M., Di Nardo, P., Licocchia, S., Traversa, E., 2010. Multiscale three-dimensional scaffolds for soft tissue engineering via multimodal electrospinning. *Acta Biomater.* 6, 1227–1237.
- Sung, H.J., Meredith, C., Johnson, C., Galis, Z.S., 2004. The effect of scaffold degradation rate on three-dimensional cell growth and angiogenesis. *Biomaterials* 25, 5735–5742.
- Tamayol, A., Akbari, M., Annabi, N., Paul, A., Khademhosseini, A., Juncker, D., 2013. Fiber-based tissue engineering: progress, challenges, and opportunities. *Biotechnol. Adv.* 31, 669–687.
- Thangawng, A.L., Howell, P.B., Richards, J.J., Erickson, J.S., Ligler, F. S., 2009. A simple sheath-flow microfluidic device for micro/nanomanufacturing: fabrication of hydrodynamically shaped polymer fibers. *Lab Chip* 9, 3126–3130.
- Tiwari, S.K., Tzezana, R., Zussman, E., Venkatraman, S.S., 2010. Optimizing partition-controlled drug release from electrospun core-shell fibers. *Int. J. Pharm.* 392, 209–217.
- Vunjak-Novakovic, G., Altman, G., Horan, R., Kaplan, D.L., 2004. Tissue engineering of ligaments. *Annu. Rev. Biomed. Eng.* 6, 131–156.
- Yim, E.K.F., Wan, A.C.A., Le Visage, C., Liao, I.C., Leong, K.W., 2006. Proliferation and differentiation of human mesenchymal stem cell encapsulated in polyelectrolyte complexation fibrous scaffold. *Biomaterials* 27, 6111–6122.
- Yoo, I., Song, S., Yoon, B., Kim, J.-M., 2012. Size-controlled fabrication of polydiacetylene-embedded microfibers on a microfluidic chip. *Macromol. Rapid Commun.* 33, 1256–1261.
- Yoo, I., Song, S., Uh, K., Lee, C.W., Kim, J.-M., 2015. Size-controlled fabrication of polyaniline microfibers based on 3D hydrodynamic focusing approach. *Macromol. Rapid Commun.* 36, 1272–1276.
- Zarrin, F., Dovichi, N.J., 1985. Sub-picoliter detection with the sheath flow cuvette. *Anal. Chem.* 57, 2690–2692.